PHYSICAL REVIEW D VOLUME 37, NUMBER 5 1 MARCH 1988

# Solvable model of beam-beam effects in $e^+e^-$ colliding storage rings

Kohji Hirata
*National Laboratory for High Energy Physics, Oho-machi, Tsukuba-gun, Ibaraki-ken 305, Japan*
(Received 25 September 1987)

A solvable model is constructed for the strong-beam–strong-beam phenomenon. The model represents the extreme case where the radiation effect is quite strong. Although it does not present a quantitatively accurate description of the beam behavior for realistic ring parameters, it qualitatively well illustrates several common characteristic features of the observed phenomenon: saturation of the beam-beam parameter, universality of its saturated value, blowup of one of the beams (spontaneous symmetry breakdown), flip-flop hysteresis (cusp catastrophe), and so on.

## I. INTRODUCTION

In all high-energy $e^+e^-$ colliding storage rings, it is commonly observed[1] that although the luminosity $L$ increases as $I^2$ ($I$ being the beam current) for small $I$, $L$ becomes, at best, proportional only to $I$ when $I$ exceeds a certain critical value. This is caused by the beam-beam interaction: the motion of a particle in a bunch is much perturbed by the Coulomb force field produced by the partner bunch under the collision. Since this effect limits the achievable $L$ quite strongly, understanding of the phenomenon has been one of the most important subjects in accelerator theory.[2]

Although the appearances of the phenomenon are complicated and machine dependent to some extent, there are undoubtedly some common features.[1] The most remarkable are the saturation of the so-called tune-shift (or beam-beam) parameter and the universality of its saturated value.

Though there have been many studies, experimental, theoretical, and computational, understanding is still in a primitive stage. One great advance, however, was made recently. Various computer simulations, that is, multiparticle tracking, showed us[3–5] that the phenomenon can certainly be explained in terms only of the usual elements of accelerator only theory. With the ordinary factors of accelerator theory only, multiparticle tracking could reproduce many of the characteristic features of the phenomena. We do not now have to be anxious about unknown factors. For practical purposes, at this stage, multiparticle tracking seems to be the most reliable, though its reliability is limited by the ability of available computers.

On the other hand, theoretical understanding of the observed phenomena and even that of the multiparticle tracking result is far from sufficient. Since the underlying mechanism seems to be composed of simple and well-known processes, we can write a fairly accurate set of equations for the present problem. In particular, there are characteristic points which should be taken into account.

*Point 1 (Hamiltonian dynamics).* The beam-beam force can be described by a nonlinear Hamiltonian. As the perturbation theory suggests, there will be many nonlinear resonances. In addition, since the force acts at some discrete points in a ring (time dependent), this is a nonintegrable Hamiltonian system.[6] It follows that the particle motion can be chaotic when the current becomes large. In this case, perturbation theory is not reliable.

*Point 2 (radiation effect).* Because of synchrotron radiation, there is a strong damping mechanism for the transverse (and longitudinal) oscillations. At the same time, a strong diffusion mechanism is also present. The radiation effect strongly perturbs the Hamiltonian dynamics.

*Point 3 (strong-strong effect).* The beam-beam force acting on a particle in a bunch is determined by the transverse particle distribution of the other bunch under the collision. At the same time, the distribution function of the bunch is much influenced by the beam-beam force. We, thus, have to find the distribution functions of both the beams and the beam-beam force acting on the individual particles consistently and simultaneously.

Most of the previous theoretical works[7] studied point 1 only (the so-called strong-weak picture). Even when one of the beams is much weaker than the other, this picture does not seem to illustrate the essential features of the phenomenon in $e^+e^-$ rings where point 2 is also important. Further, point 3 must not be ignored for both proton and electron rings. In fact, probably the most extended and successful survey along this line of thought[8] showed an estimation one order of magnitude weaker for the beam-beam effect for proton machines.

There seems at present no analytical tool to attack all of the points altogether satisfactorily. Such a set of equations is too complicated to treat analytically. At the present stage of understanding, the most important thing is to obtain a gross picture of what is happening in the colliding beams. For this purpose, it will be quite valuable and convenient to have a simple analytical model which illustrates some of the qualitative features of the observed phenomenon. Here, the "model" need not be fully realistic: a model is different from a theory. On the contrary, if possible, such a model must exaggerate the most important points, ignoring other secondary factors. Such models have helped physicists to acquire ideas of complicated phenomena. Recently, one such

 

solvable model was constructed for another but similar problem:[9] bunch lengthening by localized wake-force sources. The model showed good qualitative agreement with multiparticle tracking. It seems natural to extend the method to the present problem.

In this paper we will construct a model for the beam-beam phenomenon and study its properties. This problem is more complicated than that of Ref. 9. It seems convenient here to summarize the fundamental policy of the model construction and some of the characteristics of the model. All of the points stated above should be incorporated. The stress, however, is on points 2 and 3, which I think are the most important in this case: the model will represent the case where the radiation effect (point 2) is quite strong. This is opposite to the so-called strong-weak picture, which represents the case where the radiation effect is weak or absent. We should, in addition, consider a case where the beam-beam force is strong, i.e., the case where the perturbation theory does not work well. The resulting model will show (a) the saturation of the beam-beam parameter, which is equivalent to $L \propto I$ for large $I$, (b) blowup of one beam above a certain current even when the dynamics is set completely symmetric between two beams, and (c) existence of an unnatural stable equilibrium state in which the strong beam is blown up but the weak beam is not blown up (flip-flop hysteresis).[10]

This paper is an extended version of some of the previous short reports.[11–13] This paper is arranged as follows. In the next section, some basic principles will be given. Then in Sec. III we will construct the model. Since the model is rather complicated, we will consider a simplified case in Sec. IV, where both the beams behave symmetrically. In Sec. V we shall extend the model so that beams can move independently, but the dynamics shall be symmetric between beams. The effect of the asymmetry of dynamics will be considered in Sec. VI. The last section will be devoted to discussions and a summary. Some of the miscellaneous discussions will be relegated to the Appendixes.

## II. BASIC PRINCIPLES

Let us begin by summarizing some well-known factors. For simplicity, consider a storage ring with one interaction point (IP) and a pair of bunches ($e^+$ and $e^-$) running in opposite directions, each containing $N$ particles. In order to calculate the beam-beam kick, we will assume that the bunches are round Gaussian in coordinate space; the distribution function for the $e^\pm$ bunch is

$$\rho_\pm(x,y)=G_r(\sqrt{x^2+y^2};\sigma) , \tag{2.1}$$

where

$$G_r(r;a)=\frac{1}{2\pi a^2}\exp\left[-\frac{r^2}{2a^2}\right] , \tag{2.2}$$

and $x$ ($y$) is the horizontal (vertical) displacement and $\sigma$ the standard deviation. Since everything goes parallel, we will consider horizontal motion only.

The beam-beam kick felt by an individual particle in a bunch now can be expressed as[2]

$$\Delta x'=-\frac{2Nr_e}{\gamma}\frac{1}{x}\left[\exp\left[-\frac{x^2}{2\sigma^2}\right]-1\right] . \tag{2.3}$$

Here $x'$ is the slope of the displacement, $r_e$ the classical electron radius, and $\gamma$ the relativistic Lorentz factor of the bunch.

It is remarkable that, when $x \simeq 0$, the beam-beam kick is parametrized as

$$\Delta x' \simeq -\frac{1}{\beta_{\rm IP}}4\pi\xi x , \tag{2.4}$$

where $\beta_{\rm IP}$ is the horizontal betatron function at the IP. Here $\xi$ is the beam-beam parameter:

$$\xi=\frac{r_e}{4\pi\gamma}\frac{N\beta_{\rm IP}}{\sigma^2} . \tag{2.5}$$

The incoherent linear tune shift $\Delta_\nu$ due to the beam-beam interaction is given by

$$\cos(\mu+\Delta_\mu)=\cos\mu-2\pi\xi\sin\mu , \tag{2.6}$$

where $\mu=2\pi\nu$ (so that $\Delta_\mu=2\pi\Delta_\nu$) and $\nu$ is the unperturbed tune.

Let us give some phenomenology of the beam-beam effects. To be most general, from now on we consider an asymmetrical situation between two beams: we introduce, for the $e^\pm$ bunch, $N_\pm$ as the number of particles, $\gamma_\pm$ the $\gamma$ factor, and $\sigma_\pm$ the beam size at the IP. These asymmetries can occur artificially or spontaneously. The controllable parameters are the nominal (or unperturbed) beam-beam parameters $\eta_+$ and $\eta_-$ defined by

$$\eta_\pm=\frac{N_\mp r_e}{4\pi\gamma_\pm\epsilon} , \tag{2.7}$$

where $\epsilon$ is the nominal (i.e., without beam-beam effect) emittance which can be regarded as the same for either beam. The nominal beam-beam parameters are, say, $\xi$ without beam-beam phenomenon. Correspondingly, we introduce an asymmetry parameter $\chi$ and the effective nominal (i.e., without asymmetry) beam-beam parameter $H$ as

$$\chi=\frac{\eta_-}{\eta_+}=\frac{\gamma_+N_+}{\gamma_-N_-} , \tag{2.8}$$

$$H=\frac{\eta_++\eta_-}{2}=\frac{r_e}{8\pi\epsilon}\left[\frac{N_+}{\gamma_-}+\frac{N_-}{\gamma_+}\right] . \tag{2.9}$$

Conversely, we have

$$\eta_+=\frac{2}{1+\chi}H,\quad \eta_-=\frac{2\chi}{1+\chi}H . \tag{2.10}$$

Without any asymmetry, $H$ reduces to $\eta_+=\eta_-$. We call a situation where $\chi \gg 1$ (or $\chi \ll 1$) a strong-weak case.

The most important observable (this term has nothing to do with quantum mechanics but is related to the monitoring system) quantity is the luminosity

$$L=\frac{N_+N_-f_r}{4\pi\beta_{\rm IP}E} , \tag{2.11}$$

where $f_r$ is the revolution frequency and $E$ is the

effective emittance defined by

$$E=\frac{\sigma_+^2+\sigma_-^2}{2\beta_{\rm IP}} . \tag{2.12}$$

A corresponding observable quantity is the effective beam-beam parameter defined by

$$\Xi=\frac{r_e}{8\pi E}\left[\frac{N_+}{\gamma_-}+\frac{N_-}{\gamma_+}\right] . \tag{2.13}$$

Without any asymmetry, $\Xi$ reduces to $\xi$. Without the beam-beam effect, $\xi$ reduces to $\eta$. We can measure $\Xi$ either from the luminosity as

$$\Xi=\frac{L}{L_0}H=\frac{\epsilon}{E}H=\frac{N_+\gamma_++N_-\gamma_-}{N_+N_-\gamma_+\gamma_-}\frac{r_e\beta_{\rm IP}}{2f_r}L , \tag{2.14}$$

or from the tune measurement.[14–18] Here $L_0$ is the nominal luminosity defined by Eq. (2.11) with $E$ replaced by $\epsilon$. Without the beam-beam phenomenon, the luminosity will be $L_0$, which is proportional to $I^2$.

When $H$ (and thus current $I$) becomes large, however, the luminosity becomes not proportional to $H^2$; it shows a saturation of $\Xi$ or some more extreme behavior. It is almost certain that it is $E$ that is affected by the beam-beam force. The aim of the model, developed below, should thus be to give a relation between $H$ (and $\chi$) and $\Xi$ (or $E$).

In order to describe the motion of an individual particle, it is convenient to use the following canonical set of variables:

$$X=\frac{x}{\sqrt{\beta}},\quad P=\frac{\alpha x+\beta x'}{\sqrt{\beta}} . \tag{2.15}$$

It is useful to define moments

$$M^{\pm}_{ijk}\ldots=\langle X_iX_jX_k\cdots\rangle_{\pm} , \tag{2.16}$$

where $\langle\ \rangle_{\pm}$ is the average over the $e^{\pm}$ bunch and

$$X_1\equiv X,\quad X_2\equiv P .$$

In particular, $M_{11}$ is the so-called emittance. Let us define the ratio and average of $M^{\pm}_{11}$:

$$R=\frac{M^-_{11}}{M^+_{11}},\quad E=\frac{M^-_{11}+M^+_{11}}{2} , \tag{2.17}$$

the latter being nothing but the effective emittance defined before.

The effect of the synchrotron radiation can be expressed by two parameters: $\epsilon$ for diffusion and

$$T_\epsilon\equiv\frac{\text{transverse damping time}}{\text{revolution time}} \tag{2.18}$$

for damping. The latter is the inverse of the damping decrement introduced by Keil and Talman[19] as a good parameter for comparing various electron storage rings.

Now, the changes of the canonical variables during one turn can be written as successive operations of the following three mappings.

**O** (oscillation):

$$\begin{pmatrix}X'\\P'\end{pmatrix}=U\begin{pmatrix}X\\P\end{pmatrix} ,$$

where

$$U=\begin{bmatrix}\cos\mu & \sin\mu\\ -\sin\mu & \cos\mu\end{bmatrix} . \tag{2.19}$$

**B** (beam-beam force ):

$$X'=X,\quad P'=P+K_\pm F_\pm(X) ,$$

where

$$K_\pm=8\pi\epsilon\eta_\pm , \tag{2.20}$$

$$F_\pm(X)=\frac{1}{X}\left[\exp\left[-\frac{X^2}{2M^\mp_{11}}\right]-1\right] . \tag{2.21}$$

**R** (radiation):

$$X'=X,\quad P'=\lambda P+\sqrt{(1-\lambda^2)\epsilon}\,\hat{r} ,$$

where $\lambda$ is the damping rate defined by

$$\lambda=\exp(-2/T_\epsilon) \tag{2.22}$$

and $\hat{r}$ is a noise with unit standard deviation. Without **B**, $M^{\pm}_{ij}$ approaches $\epsilon\delta_{ij}$ ($\delta_{ij}$ is the Kronecker $\delta$ symbol) in roughly $T_\epsilon$ turns.

In the above we have treated the effect of radiation as if it works at one point in a ring. Since this effect belongs essentially to the linear dynamics, it brings no unphysical results. In fact, in the multiparticle tracking, this is the usual technique for reducing the computational time.

## III. MAPPING EQUATIONS FOR MOMENTS

All of the information of the beams is contained in the distribution function in the phase space, $\psi_\pm(X,P)$ for the $e^\pm$ bunch. The distribution function is equivalent to the set of all the moments $M^\pm_{ijk}\ldots$. All of the moments mix with each other through the beam-beam force. That is, any moment is influenced by all of the moments of the other beam. Clearly, it is impossible to track all the moments. We are forced to make some simplifications.

We assume that the dipole moment $M_i$ is stable and thus negligible. The most important moment, then, is $M_{ij}$. Thus, let us track the changes of only $M^\pm_{ij}$ under the mappings

$$\cdots\rightarrow\mathbf{B}\rightarrow\mathbf{R}\rightarrow\mathbf{O}\rightarrow\cdots .$$

The changes of $M_{ij}$ under **O** and **R** are straightforwardly obtained as

$$\mathbf{O}:\ M^{\pm\prime}_{ij}=(UM_\pm U^t)_{ij} ,$$

$$\mathbf{R}:\ M^{\pm\prime}_{11}=M^\pm_{11},\quad M^{\pm\prime}_{12}=\lambda M^\pm_{12} ,$$

$$M^{\pm\prime}_{22}=\lambda^2M^\pm_{22}+(1-\lambda^2)\epsilon .$$

Here $U^t$ is the transpose of $U$. Note that the effect of **R** can now be treated as a deterministic process. The change under **B** is described as

$$\mathbf{B}:\ M^{\pm\prime}_{11}=M^\pm_{11},\quad M^{\pm\prime}_{12}=M^\pm_{12}+K_\pm\langle XF_\pm(X)\rangle_\pm ,$$

$$M^{\pm\prime}_{22}=M^\pm_{22}+2K_\pm\langle PF_\pm(X)\rangle_\pm+K^2_\pm\langle F_\pm(X)^2\rangle_\pm .$$

To evaluate $\langle\ \rangle$'s appearing in **B** we have to know $\psi_\pm$.

At this stage, some approximation is inevitable. From many possibilities, let us choose the Gaussian approximation:

$$\psi(X_1,X_2)_\pm=\frac{1}{2\pi\sqrt{\det M_\pm}}\exp[-\tfrac{1}{2}(M_\pm^{-1})_{ij}X_iX_j]\ , \tag{3.1}$$

where summation over indices (from 1 to 2) is assumed. The Gaussian distribution can be reconstructed from the second-order moments only. When the beam-beam force is weak or even when the force is strong but the radiation effect is also strong enough, $\psi$ is naturally expected to be nearly Gaussian. As discussed in Ref. 9, for the evaluation of averages, we must use $M_{ij}$ just before[20] **B**. By elementary integrations, we have

$$\langle XF_\pm(X)\rangle_\pm=A(R^{\pm1})\ , \tag{3.2}$$

$$\langle PF_\pm(X)\rangle_\pm=A(R^{\pm1})M_{12}^\pm/M_{11}^\pm\ , \tag{3.3}$$

$$\langle F_\pm(X)^2\rangle_\pm=B(R^{\pm1})/M_{11}^\pm\ , \tag{3.4}$$

where

$$A(R)=\left[\frac{R}{1+R}\right]^{1/2}-1\ , \tag{3.5}$$

$$B(R)=2\left[1+\frac{1}{R}\right]^{1/2}-\left[1+\frac{2}{R}\right]^{1/2}-1\ , \tag{3.6}$$

and $R$ is defined by Eq. (2.17).

Let us track the change of $M_{ij}$ on the Poincaré surface built just before **B**. Presumably, $\psi$ eventually falls into a steady state, which implies that $M_{ij}^\pm$ becomes periodic in one turn. It is thus interesting to find a period-one fixed point $\tilde{M}_{ij}$ on the surface. We denote $M_{ij}$ at various stages as

$$M\underset{\mathrm{B}}{\rightarrow}M'\underset{\mathrm{R}}{\rightarrow}M''\underset{\mathrm{O}}{\rightarrow}M'''\ . \tag{3.7}$$

The period-one fixed point $\tilde{M}_{ij}$ is the solution of

$$M=M'''\ . \tag{3.8}$$

After some algebra (see Appendix A) we obtain, for the fixed point,

$$\tilde{M}_{11}^{\pm}=D_\pm+(D_\pm^2+E_\pm)^{1/2}\ , \tag{3.9}$$

$$\tilde{M}_{12}^{\pm}=-\frac{\lambda}{1+\lambda}K_\pm A(\tilde{R}^{\pm1})\ , \tag{3.10}$$

$$\tilde{M}_{22}^{\pm}=\epsilon+E_\pm/\tilde{M}_{11}^{\pm}\ , \tag{3.11}$$

where

$$D_\pm=\frac{\lambda}{1+\lambda}\frac{K_\pm A(\tilde{R}^{\pm1})}{\tan\mu}+\frac{\epsilon}{2}\ , \tag{3.12}$$

$$E_\pm=K_\pm^2\frac{\lambda^2}{1-\lambda^2}\left[B(\tilde{R}^{\pm1})-\frac{2\lambda}{1+\lambda}A(\tilde{R}^{\pm1})^2\right]\ . \tag{3.13}$$

Here everything is expressed as a function of $\tilde{R}$, which in turn is a solution of the consistency condition

$$R=h(R) \tag{3.14}$$

with

$$h(\tilde{R})=\frac{\tilde{M}_{11}^{-}}{\tilde{M}_{11}^{+}}=\frac{D_-+(D_-^2+E_-)^{1/2}}{D_++(D_+^2+E_+)^{1/2}}\ . \tag{3.15}$$

The problem is reduced now to solving the consistency condition. Before entering into details, it should be noted that the numerical tracking of $M_{ij}^\pm$ shows that any $M_{ij}^\pm$ falls into $\tilde{M}_{ij}^{\pm}$ after sufficient turns. Of course, this is not assured *a priori*. In general, there can appear a period-two, for example, fixed point, chaotic behavior and so on. It is fortunate that such complicated phenomenon is not present.

Let us examine this solution. Since the solution is slightly complicated, we will start with the simplest case and proceed to more and more general cases as follows: (1) $\chi=1$ and $R=1$ (the latter condition is somewhat artificial but useful for its simplicity); (2) $\chi=1$, but $R$ is determined by the consistency condition (3.14); (3) $\chi\neq1$.

## IV. UNIVERSALITY OF THE BEAM-BEAM LIMIT

When the current becomes large, the luminosity often becomes proportional only to $I$. It implies a saturation of $\Xi$ for large, $I$. It is almost certain[1] that $E$ is enlarged from $\epsilon$ in proportion to $I$. The aim of this section is to illustrate this phenomenon. In this and subsequent sections, for the sake of simplicity, we will assume that the controllable parameters are set symmetric between two beams so that $\chi=1$ and the subscript $\pm$ for $\eta$, $K$, etc., can be omitted. In addition, in this section, we will assume that the two beams are identical ($M_{ij}^+=M_{ij}^-$ so that $R=1$), thus,

$$\begin{aligned}A&=A_1=\sqrt{2}/2-1\simeq-0.2929\ ,\\ B&=B_1=2\sqrt{2}-\sqrt{3}-1\simeq0.09638\ .\end{aligned} \tag{4.1}$$

Now $\tilde{M}_{ij}$ in Eqs. (3.9)–(3.11) are given as explicit functions of $\lambda$, $\mu$, and $H$.

From Eq. (3.9), it is easily seen that (i) when $H\ (=\eta)$ is small, $\tilde{M}_{11}=\epsilon$ and (ii) when $H$ is large enough, $\tilde{M}_{11}$ is proportional to $H$. Here, the effective emittance $E$ is just $\tilde{M}_{11}$. The effective beam-beam parameter is thus given as

$$\Xi=\frac{\epsilon H}{D_1+(D_1^2+E_1)^{1/2}}\ , \tag{4.2}$$

where $D_1$ and $E_1$ are $D_\pm$ and $E_\pm$ with $R=1$. As is easily seen, (i) when $H$ is small $\Xi=H$ and (ii) when $H$ becomes large $\Xi$ approaches a limit $\Xi_\infty$:

$$\Xi_\infty=\frac{1}{8\pi}\frac{1}{d_1+(d_1^2+e_1)^{1/2}}\ , \tag{4.3}$$

where

$$d_1=\frac{\lambda}{1+\lambda}\frac{A_1}{\tan\mu}\ , \tag{4.4}$$

$$e_1=\frac{\lambda^2}{1-\lambda^2}\left[B_1-\frac{2\lambda}{1+\lambda}A_1^2\right]\ . \tag{4.5}$$

The model thus illustrates the saturation of the beam-beam parameter, see Fig. 1, which is quite similar to the

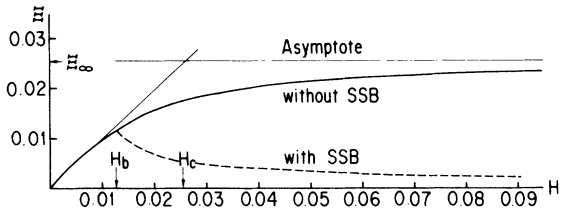


FIG. 1. The dependence of $\Xi$ on $H$. The case with the spontaneous symmetry breakdown (see Sec. V) is also shown by the dashed line. Parameters $T_\epsilon=1428$, $\nu=0.05$. Definitions of $H_c$ and $H_b$ (see Sec. V) are also illustrated. They are 0.0257 and 0.0127 for the present parameters, respectively.

simulation result of Myers (Fig. 6 of Ref. 5). As a model value we use $T_\epsilon=1428$, which is $T_\epsilon$ for the TRISTAN main ring at KEK, but multiplied by its super periodicity (four) and $\nu=0.05$ as a model value. The saturated value $\Xi_\infty$, which should be denoted as the beam-beam limit, is 0.0257 for these model values. For later convenience, let us define the critical value of $H$, $H_c\equiv\Xi_\infty$. The $\Xi$ becomes saturated at $H=H_c$. It is remarkable that $H_c$ is a function only of $\nu$ and $T_\epsilon$.

The saturated value is shown as a function of $\nu$ for some values of $T_\epsilon$ in Fig. 2. As shown in the figure, $\Xi_\infty$ blows up for $\nu\to 0^+$ and falls down for $\nu\to 0^-$. (All $\nu$ dependence repeats itself in modulo $\frac{1}{2}$.) This is due to the $\tan\mu$ factor in $d_1$: in the former case, $\Xi_\infty$ is dominated by $d_1$, while by $e_1$ in the latter case. The $\nu\to 0^+$ case is consistent with observation.[21] This result seems to imply that $\nu$ should be close to $0^+$ to obtain high $\Xi_\infty$. (However, see Sec. V.) For physically realistic $\nu$ (say $0.05<\nu<0.45$) $\Xi_\infty$ seems to be almost constant. As can also be seen from Fig. 2, the dependence of $\Xi_\infty$ on $T_\epsilon$ is quite weak: when $T_\epsilon$ is large, $\Xi_\infty$ is dominated by the $1-\lambda^2$ factor in $e_1$, which implies that $\Xi_\infty$ is proportional to $T_\epsilon^{-1/2}$ (and thus to $\gamma^{3/2}$). This seems to be consistent with an analysis of the experimental data given in Ref. 1. It is interesting to see that the same dependence was predicted by Chao[2] by a quite different consideration.

In this respect, the universality of $\Xi_\infty$ can be explained as a result of the fact that in every high-energy $e^+e^-$ colliding ring, $T_\epsilon$ has almost the same order of magnitude at its highest energy.

When there are $N_{\rm IP}$ interaction points and $N_{\rm IP}$ $e^+$ and $N_{\rm IP}$ $e^-$ bunches, $T_\epsilon$ should be multiplied by $N_{\rm IP}$ ($\nu$ is divided by $N_{\rm IP}$). It follows that

$$\Xi_\infty\propto\frac{1}{\sqrt{N_{\rm IP}}}\ , \tag{4.6}$$

which is the same prediction as that given by Wiedeman.[22]

According to Ref. 1, the linear tune-shift limit $\Delta_\nu^\infty$, defined as

$$\cos[2\pi(\nu+\Delta_\nu^\infty)]=\cos\mu-2\pi\Xi_\infty\sin\mu\ , \tag{4.7}$$

is more universal than $\Xi_\infty$. This can be explained as follows. In our model, when $\nu\to 0^+$, $\Xi_\infty$ behaves like $\cot\mu$ multiplied by a constant. From Eq. (4.7), it is easy to see that $\Delta_\nu^\infty$ is regular at this limit. In fact, $\Delta_\nu^\infty$ is quite regular (almost constant) against a variation of $\nu$, as shown also in Fig. 2. It should be noted that, when $\nu\lesssim 0.5$, $\Delta_\nu^\infty$ cannot be a real number, which corresponds to the linear instability for the coherent and incoherent dipole transverse oscillations.[17]

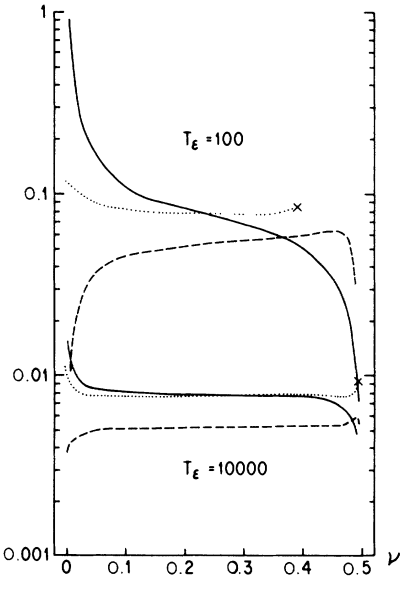


FIG. 2. The dependences of $H_c$ (solid line), $\Delta_\nu^\infty$ (dotted line), and $H_b$ (dashed line) (see Sec. V) on $\nu$. Beyond $\times$, $\Delta_\nu^\infty$ is complex.

## V. SPONTANEOUS BREAKDOWN OF THE SYMMETRY BETWEEN BEAMS

In this section, the beams are allowed to move independently ($M_{ij}^+\neq M_{ij}^i$), whereas the dynamical setup is completely symmetric between beams ($\chi=1$).

We have to solve Eq. (3.14) to find $\tilde{R}$. It is easy to see that (i) this equation has trivial solutions 0, 1, and $\infty$ and (ii) when $R$ is the root, so is $R^{-1}$. The function of $h(R)$ is illustrated in Fig. 3 for two values of $H$. When

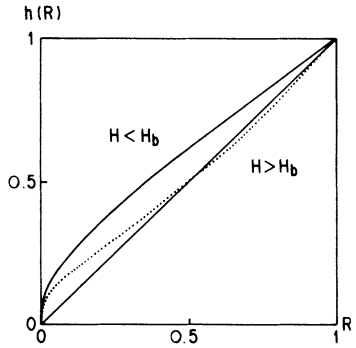


FIG. 3. The function $h(R)$ for two values of $H$: $H<H_b$ (solid line) and $H>H_b$ (dotted line).

$H$ is small, only the trivial roots 0, 1, and $\infty$ are the solutions. When $H$ becomes large, and exceeds some value, a new pair of solutions $\tilde{R}^{\pm 1}$ is born. We call such a value of $H$ as $H_b$ (the bifurcation $H$), which is an implicit function only of $\nu$ and $T_\epsilon$. By numerically tracking the mapping equations for $M_{ij}^{\pm}$, we find that (i) when $H < H_b$ the stable fixed point is uniquely given by $R = 1$ and (ii) when $H > H_b$, $R = 1$ becomes unstable and, instead the newly created roots become stable. Such a behavior is known as the pitchfork bifurcation and is illustrated in Fig. 4.

One of the two branches ($R > 1$ or $R < 1$) is chosen spontaneously. The beams prefer such an asymmetric state even if the kinematical setup is completely symmetric between beams. One of the beams is blown up unavoidably. Which beam is blown up cannot be decided. Once one beam is blown up, the other beam feels a relatively weak force so that it is never blown up. This is an analogue of the spontaneous symmetry breakdown seen in various physical systems.

When $H$ exceeds $H_b$, one of the beams is blown up rapidly. In such a case, the luminosity and $\Xi$ decrease rapidly as shown in Figs. 1 and 5. Such a rapid decrease of $\Xi$ was actually observed and reported in Ref. 14 (see Ref. 23). The dependence of $H_b$ on $\nu$ and $T_\epsilon$ is shown in Fig. 2. From the figure, $H_b$ is almost always below $H_c$ as long as $\Delta_\nu$ is real: this means that the spontaneous symmetry breakdown occurs inevitably before we reach $H = H_c$.

From the multiparticle tracking,[5] however, the actual beam behavior seems to depend more sensitively on $\nu$ so that, for some $\nu$, $H_b$ seems to be larger. We compared the model to the multiparticle tracking results in Figs. 4 and 5 (see Sec. VII B). The agreement is good at least qualitatively. In this example, the bifurcation is modest in the multiparticle tracking so that $\Xi$ actually seems to

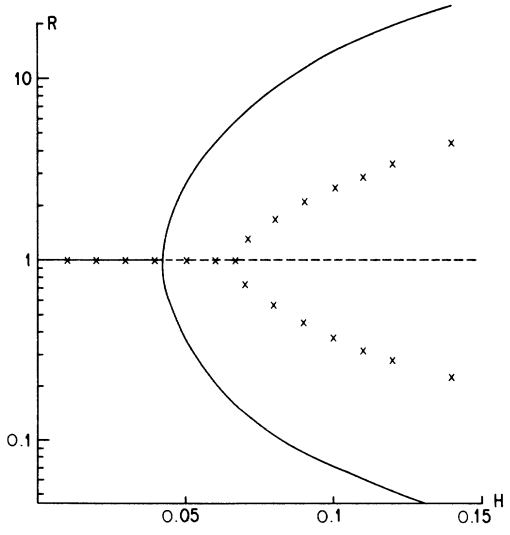


FIG. 4. The pitchfork bifurcation for the ratio of the beam size. The results of the multiparticle tracking are also shown by crosses. Parameters $T_\epsilon = 142.8$ and $\nu = 0.2$. For these parameters, $H_b = 0.0429$ and $H_c = 0.0683$.

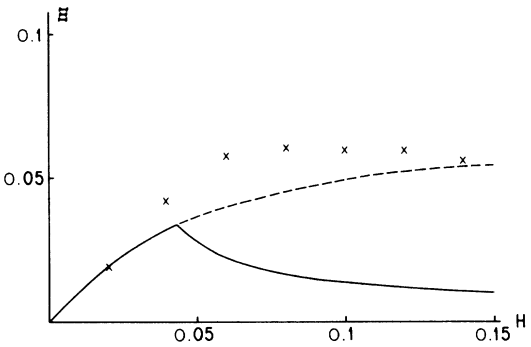


FIG. 5. The sudden decrease of $\Xi$ due to spontaneous symmetry breakdown. The dashed line corresponds to a case without spontaneous symmetry breakdown. The results of the multiparticle tracking are also shown by $\times$. Parameters $T_\epsilon = 142.8$ and $\nu = 0.2$.

be saturated. The result of the previous section can apply in such cases. For some $\nu$, the bifurcation is more sharp.[24] The effort of machine study should thus be on finding $\nu$ such that $H_b$ is considerably large and the decrease of $\Xi$ is not so rapid. Some information can be drawn from the model. In the model, $H_b$ falls for $\nu \to 0^+$: the opposite to the dependence of $H_c \equiv \Xi_\infty$. It is thus dangerous to choose $\nu$ very close to $0^+$, even if $\Xi_\infty$ is large there. In fact, the result of the multiparticle tracking[5] shows that such $\nu$ is not good for the luminosity and $\nu \simeq 0.2$ will be better.

It is interesting to see the changes of the beam sizes $M_{11}^{\pm}$ as $H$ increases. In Fig. 6 we show it along with the result of the multiparticle tracking. After the bifurcation, $M_{11}$ of one of the beams becomes almost $\epsilon$, the nominal value. This situation is quite similar to the strong-weak case, which will be discussed in Sec. VII C. Assume that the $e^+$ beam is very blown up so that $R$ is quite small. Now, we have $RM_{11}^{+} \simeq \epsilon$. From Eqs. (3.5)–(3.6), it is clear that $A(R)$ and $B(R)/M_{11}^{+}$ become quite small. Then from Eqs. (3.2)–(3.4) we see that the effect of the beam-beam kick becomes small for the $e^+$ beam. As for the $e^-$ beam, the effect becomes indifferent to the encountering beam. As a result, $M_{11}^{-}$ is

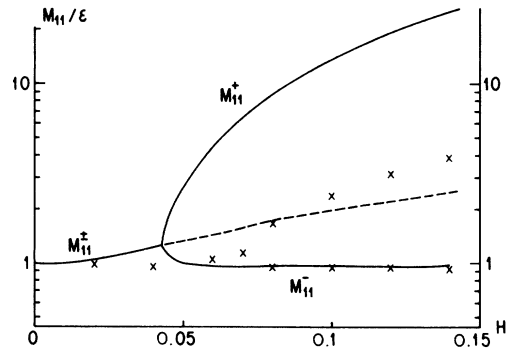


FIG. 6. The beam sizes $M_{11}^{\pm}$ as functions of $H$. The results of the multiparticle tracking are also shown by crosses. Parameters $T_\epsilon = 142.8$ and $\nu = 0.2$.

a little smaller than the nominal value, which is due to the weak focusing effect from the other beam. Thus after the bifurcation the effect of the beam-beam interaction becomes weak. Clearly, this fact is closely related to the reason why the spontaneous symmetry breakdown occurs. This effect comes from the nature of the beam-beam force. As stressed by Chao,[2] the force decreases exponentially outside the central region of the encountering bunch. Such a thing does not occur for a polynomial-like force. Expansion of the force in Taylor series, often used in the perturbative approach, thus does not work. See also Sec. VII E.

## VI. CUSP CATASTROPHE AND FLIP-FLOP HYSTERESIS

In this section, the setup is asymmetric between beams ($\chi \neq 1$). The roots of Eq. (3.14) are illustrated in Fig. 7 with some value of $\chi$. The case that $\chi=1$ is already discussed. When $\chi$ is even slightly different from 1, the curve changes in a topologically inequivalent manner. That is, the bifurcation behavior for $\chi=1$ is structurally unstable.[25] (When $\chi$ is very close to 1, however, it is actually difficult to experimentally distinguish these two cases.) As indicated in the figure, we define $H_b(\chi)$ as $H$ giving the bifurcation (fold) point. By numerically tracking the mapping for $M_{ij}^{\pm}$ with fixed $\chi$, we can confirm that (i) when $H \leq H_b(\chi)$ there is only one stable solution and (ii) when $H > H_b(\chi)$ there are two stable solutions (solid lines) and one unstable solution (dashed line). (We ignore solutions 0 and $\infty$.)

The case $\chi > 1$ means that the $e^+$ beam is stronger than the $e^-$ beam (more energetic or more intense). It is thus quite natural to expect that the $e^-$ beam is blown up ($\tilde{R} > 1$). However, there can be a stable state where the opposite occurs. Let us call the former case "natural" and the latter "unnatural." Let the state be unnatural with some $\chi$, then as $H$ decreases, the state "jumps" to the natural one at $H = H_b(\chi)$.

In Fig. 8, $\tilde{R}$ is shown as a function of $\chi$ with $H$ fixed. In Figs. 7 and 8, an unphysically large value of $\chi$ is used for illustrative clarity. For $H > H_b(1)$ and $\chi \simeq 1$, there are two stable values of $\tilde{R}$ (they correspond to the two branches discussed in the previous section), while there can be only one stable state when $\chi$ is to some extent different from 1. Let the state be at point $A$ in Fig. 8. If $\chi$ decreases, the state is moved to the point $B$ and then to $C$. A further decrease of $\chi$ will force the state jump from $C$ to $D$, and then move to $E$. After that, when $\chi$ increases, the state follows the different path: $E \rightarrow D \rightarrow F \rightarrow B \rightarrow A$. The oscillation of $\chi$ around 1 with enough amplitude, therefore, results in a hysteresis loop in the $R$-$\chi$ plane. [The necessary amplitude depends on $H - H_b(\chi=1)$.] We can actually control $\chi$ to some extent. One possible way is to control $\gamma_{\pm}$ by controlling the relative phase of rf acceleration as reported in Ref. 10.

This illustrates qualitatively what is observed in the SLAC $e^+e^-$ storage ring SPEAR (Ref. 10). From Ref. 10, it is almost certain that asymmetry between beams is responsible for the hysteresis, though what asymmetry is the most effective is not well known. In the present model, the controllable parameters are only $\gamma_{\pm}$ and $N_{\pm}$. This, however, does not restrict the generality of its results, since the behavior shown thus far is not a special one, but rather a generic one. According to the general theory of bifurcation,[26] only this type of behavior is structurally stable for the system with two parameters. (In our model, the parameters are $H$ and $\chi$.) We thus expect that the same will occur also from other types of

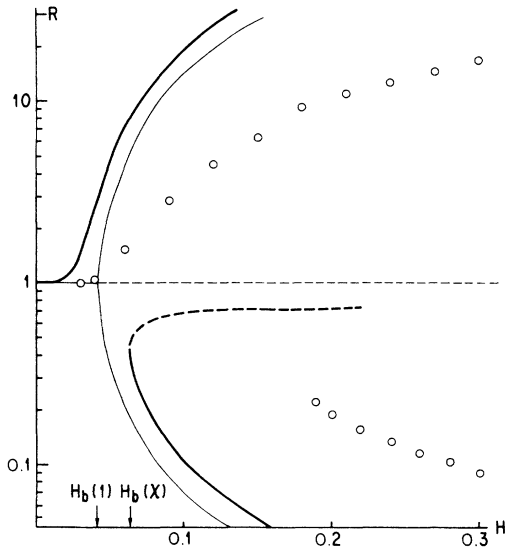


FIG. 7. The roots of $R = h(R)$: $\tilde{R}$ as a function of $H$ with $\chi=1$ (thin line) and with $\chi=1.5$ (bold line). Solid lines are stable, while dashed lines are unstable. The results of the multiparticle tracking are also shown (circle). The definition of $H_b(\chi)$ is indicated. Parameters $T_\epsilon = 142.8$ and $\nu = 0.2$.

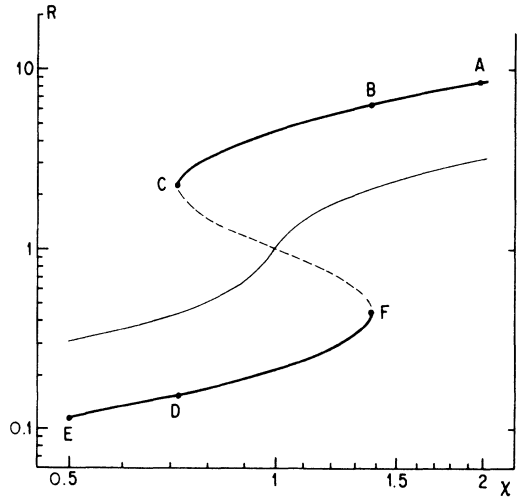


FIG. 8. The roots $\tilde{R}$ as a function of $\chi$ with $H=0.06$ [above $H_b$ ($\chi=1$), bold line] and $H=0.04$ [below $H_b$ ($\chi=1$), thin line]. Solid lines are stable, while dashed lines are unstable. Parameters $T_\epsilon = 142.8$ and $\nu = 0.2$.

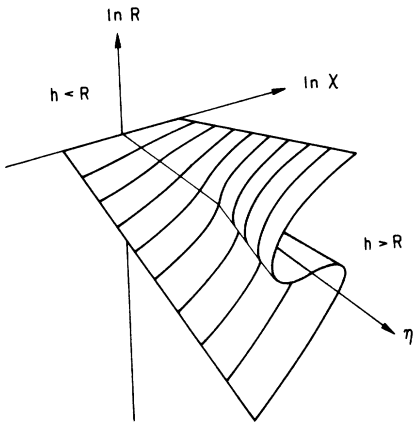


FIG. 9. Conceptual illustration of the root $\tilde{R}$ as a function of $H$ and $\chi$. The well-known diagram of the cusp catastrophe.

asymmetry which cannot be incorporated in this model. An overview is illustrated in Fig. 9. The sheet shown here corresponds to $R=h(R)$. The figure is well known as the diagram of the cusp catastrophe. There are many systems which have the same state diagram.[27,28]

This model thus implies that the flip-flop hysteresis is generic in $e^+e^-$ colliding rings in which (i) $H$ can be larger than $H_b(1)$ and (ii) $\chi$ is to some extent controllable adiabatically (i.e., continuously and slowly compared to the damping time). Since, actually, $\chi$ cannot be changed so much, the hysteresis is possible only when $H$ is slightly larger than $H_b(1)$; even a small asymmetry can cause a considerable hysteresis, because $\tilde{R}$ rises rapidly at $H=H_b$ when $\chi=1$. In general, the unnatural state provides larger luminosity than the natural state. It is thus of practical importance to find the most effective source of asymmetry and to control it so that the system is always in the unnatural state when $H>H_b(1)$: of course, the first effort should be on finding a tune where the state $R=1$ can be maintained for larger $H$, as discussed in the previous section.

We compare the results of the model to those of the multiparticle tracking in Fig. 7. (See Sec. VII B.) When we start from small $H$ and increase it, the state follows the natural path. When we start from the unnatural initial state with large enough $H$, as $H$ decreases the state follows the unnatural path and jumps to the natural state at some point. The results of multiparticle tracking are quite consistent with our model. It is, however, observed that the statistical quantities $M_{ij}^{\pm}$, when in the unnatural state, fluctuate much at $H \gtrsim H_b(\chi)$. It is natural since the stable state is then quite close to the unstable fixed point. When $H$ is decreased a little, the state moves to the natural one in roughly $10T_\epsilon$ turns. The result of the multiparticle tracking seems to much depend on the number of particles in this region. Thus, for realistic $\chi$, it seems quite difficult to decide $H_b$ by the multiparticle tracking accurately. In the figure $2\times10^4$ particles in each beam are used to identify $M_{ij}^{\pm}$ near $H_b(\chi)$.

## VII. DISCUSSIONS

Based on the arguments given thus far, we shall introduce some miscellaneous discussions.

### A. Flat-Gaussian limit

We have assumed that the beams are round at the collision point (round-beam limit) for the sake of simplicity. In almost all electron colliding rings, however, the beams are flat in shape. When we assume that the beams are much wider than they are high so that the horizontal motion can reasonably be neglected, we can construct another model (flat-beam limit).[29]

In the present case, the beam-beam kick felt by an individual particle can approximately be written as[30]

$$\Delta x'_{\pm}=-\frac{N_{\mp}r_e}{\gamma_{\pm}}\frac{\sqrt{2\pi}}{\sigma_{x\mp}}\exp\left[-\frac{x_{\pm}^2}{2\sigma_{x\mp}^2}\right]\mathrm{erg}\left[\frac{x_{\pm}}{\sqrt{2}\sigma_{x_{\mp}}}\right], \tag{7.1}$$

$$\Delta y'_{\pm}=-\frac{N_{\mp}r_e}{\gamma_{\pm}}\frac{\sqrt{2\pi}}{\sigma_{x\mp}}\exp\left[-\frac{x_{\pm}^2}{2\sigma_{x\mp}^2}\right]\mathrm{erf}\left[\frac{y_{\pm}}{\sqrt{2}\sigma_{y\mp}}\right], \tag{7.2}$$

where $x$ ($y$) is the horizontal (vertical) displacement, $x'$ ($y'$) its slope, and

$$\mathrm{erf}(x)=\frac{2}{\sqrt{\pi}}\int_0^x\exp(-t^2dt)\,, \tag{7.3}$$

$$\mathrm{erg}(x)\equiv -i\,\mathrm{erf}(ix)\,. \tag{7.4}$$

Although this simplified kick is not symplectic, we can use it when considering only the vertical motion.

The nominal beam-beam parameter, instead of Eq. (2.7), for the $e^{\pm}$ bunch is defined by

$$\eta_{\pm}=\frac{r_eN_{\mp}}{2\pi\gamma_{\pm}}\frac{\beta_y^0}{\sigma_x^0(\sigma_x^0+\sigma_y^0)}=\frac{N_{\mp}r_e}{2\pi\gamma_{\pm}}\left[\frac{\beta_y^0}{\beta_x^0}\right]^{1/2}\frac{1}{(\epsilon_x\epsilon_y)^{1/2}}\,, \tag{7.5}$$

where $\sigma_x^0$ ($\sigma_y^0$) is the horizontal (vertical) nominal beam size, $\beta_x^0$ ($\beta_y^0$) is the betatron function at IP, and $\epsilon_x$ ($\epsilon_y$) is the horizontal (vertical) nominal emittance.

The asymmetry parameter $\chi$ and $H$ are defined by the same expressions as Eq. (2.8) and (2.9). The beam-beam parameter $\Xi$ now should be

$$\Xi=\frac{L}{L_0}H=\left[\frac{\epsilon_y}{E_y}\right]^{1/2}H\,, \tag{7.6}$$

where

$$E_y=\frac{\sigma_{y+}^2+\sigma_{y-}^2}{2\beta_y^0} \tag{7.7}$$

is the extension of $E$, Eq. (2.12).

Let us track the moments

$$\Lambda_{ij}^{\pm}\equiv\langle Y_iY_j\rangle_{\pm}$$

in vertical phase space $(Y_1, Y_2)$, where $Y_1$ $(Y_2)$ is the usual canonical coordinate (momentum). Each particle in a bunch feels at the IP the beam-beam force from the other bunch:

$$\Delta Y_2^{\pm} = -(2\pi)^{3/2}\eta_{\pm}\sqrt{\Lambda_{11}^{\mp}}\left\langle \exp\left[-\frac{x^2}{2\sigma_x^2}\right]\right\rangle \mathrm{erf}\left[\frac{Y_1}{\sqrt{2\Lambda_{11}^{\mp}}}\right]. \tag{7.8}$$

Here we assume that the horizontal beam sizes are not affected by the beam-beam force so that the average $\langle\ \rangle$ in the above is $1/\sqrt{2}$.

The change of $\Lambda_{ij}^{\pm}$ for one turn can be tracked by the successive application of the mappings $\cdots\rightarrow\mathbf{B}\rightarrow\mathbf{R}\rightarrow\mathbf{O}\rightarrow\cdots$. The **R** and **O** are the same as the case of the round-beam limit, while **B** is now given by

$$\mathbf{B}:\ \Lambda_{11}^{\pm\prime}=\Lambda_{11}^{\pm},\quad \Lambda_{12}^{\pm\prime}=\Lambda_{12}^{\pm}+2\kappa_{\pm}A(R^{\pm 1})[\Lambda_{11}^{\pm}]^{1/2},$$
$$\Lambda_{22}^{\pm\prime}=\Lambda_{22}^{\pm}+4\kappa_{\pm}A(R^{\pm 1})\Lambda_{12}^{\pm}[\Lambda_{11}^{\pm}]^{-1/2}+4\kappa_{\pm}^2 B(R^{\pm 1}),$$

where

$$R=\frac{\Lambda_{11}^{-}}{\Lambda_{11}^{+}},\quad A(R)=-\frac{1}{[2\pi(1+R)]^{1/2}},$$
$$B(R)=\frac{1}{4}-\frac{1}{\pi}\arcsin\left[\frac{R}{2(1+R)}\right]^{1/2},$$

and

$$\kappa_{\pm}=2\pi^{3/2}\sqrt{\epsilon_y}\eta_{\pm}.$$

Here $B(R)$ comes from the evaluation of $\langle$(beam-beam kick)$^2\rangle$ (Ref. 31).

As in the case of the round-beam limit, the mappings have (period-one) fixed point $\tilde{\Lambda}_{ij}^{\pm}$ on a Poincaré surface of the section built just before **B**:

$$\tilde{\Lambda}_{11}^{\pm}=[D_{\pm}+(\epsilon_y+D_{\pm}^2+E_{\pm})^{1/2}]^2,$$
$$\tilde{\Lambda}_{12}^{\pm}=-\frac{2\lambda}{1+\lambda}\kappa_{\pm}A(\tilde{R}^{\pm 1})\sqrt{\tilde{\Lambda}_{11}^{\pm}},$$
$$\tilde{\Lambda}_{22}^{\pm}=\epsilon_y+E_{\pm},$$

where

$$D_{\pm}=\kappa_{\pm}\frac{2\lambda}{1+\lambda}A(\tilde{R}^{\pm 1})\frac{1}{\tan\mu},$$
$$E_{\pm}=\kappa_{\pm}^2\frac{4\lambda^2}{1-\lambda^2}\left[B(\tilde{R}^{\pm 1})-\frac{2\lambda}{1+\lambda}A(\tilde{R}^{\pm 1})^2\right],$$

and $\tilde{R}$ is a root of the equation $R=h(R)$,

$$h(R)=\frac{[D_-+(\epsilon_y+D_-^2+E_-)^{1/2}]^2}{[D_++(\epsilon_y+D_+^2+E_+)^{1/2}]^2}. \tag{7.9}$$

Expressions given thus far are natural extensions of those given for the round-beam limit. Qualitative features of the model are the same. This is a little surprising: for the saturation of $\Xi$, $M_{11}$ (round-beam limit) should be proportional to $I$ while $\Lambda_{11}$ (flat-beam limit) should be proportional to $I^2$. The fact that these two oppositely extreme cases agree well implies that the same things can be expected for general cases.[32]

### B. Multiparticle tracking

We have constructed a solvable model which seems to illustrate strange things in the beam-beam phenomena. To see that the results of the model do not come from improper approximations, it is useful to do the multiparticle tracking for the mappings defined in Sec. II. We use at least 2000 test particles in each beam and track the changes of these particles for more than $10T_{\epsilon}$ turns. Our model value for $T_{\epsilon}$ is one order of magnitude smaller than the realistic one. This is used only because of the relative ease for multiparticle tracking. For realistic $T_{\epsilon}$ we should use, at least, one order more number of turns and presumably one order more test particles. Here we use the Gaussian approximation only to evaluate the beam-beam force, which is the same as Myers.[5] The results have been shown in figures and discussed in some sections.

It is remarkable that our model and the results of the multiparticle tracking agree well qualitatively (topologically). That is, though the quantitative agreement is not good, the results of the multiparticle tracking shows (1) the saturation of $\Xi$ for some $\nu$, (2) the spontaneous symmetry breakdown and rapid decrease of $\Xi$, and (3) flip-flop hysteresis. In some tunes, the quantitative agreement is particularly not good. (See Sec. VII C.) In general, $H_b$ is more dependent on $\nu$ than the model.

As will be discussed in the following two subsections, the quantitative agreement between the results of our model and the multiparticle tracking is good for small $T_{\epsilon}$. Even for a larger value of $T_{\epsilon}$, the "topological" agreement is still good. Some of the examples can be seen in Ref. 12.

We thus can conclude that our model can illustrate the characteristic behavior of the beams at least within the simplification adopted in the multiparticle tracking.

### C. Strong-weak case

The strong-weak picture without the radiation effect is well studied. There are several detailed studies with the radiation effect.[33–35] It seems, however, quite difficult to extend these works to the strong-strong case. It is interesting, in turn, to apply our model to the strong-weak case.

Let us assume that the $e^+$ bunch is much stronger than the $e^-$ bunch so that $\chi$ is almost $\infty$. In this case, $H\simeq\eta_-/2$ [see Eq. (2.9)] and $M_{ij}^{+}=\epsilon\delta_{ij}$. We will write $\eta_-$ and $M_{ij}^{-}$ simply as $\eta$ and $M_{ij}$, respectively, in this subsection.

All we have to do is to redefine $R$, Eq. (2.17), as

$$R=\frac{M_{11}}{\epsilon} \tag{7.10}$$

and $h(R)$, Eq. (3.15), as

$$h(\tilde{R})=\frac{\tilde{M}_{11}}{\epsilon}=\frac{D_-+(D_-^2+E_-)^{1/2}}{\epsilon}. \tag{7.11}$$

The period-one fixed point can be obtained numerically and is shown as a function of $\eta$ in Fig. 10 together with the results of the multiparticle tracking for comparison. Without the radiation effect, that is, only with point 1, the generic behavior of the Poincaré mapping is well known.[7] The resonance overlap occurs at $\eta=\eta_s$, which is[36] $\simeq 0.17$ for $\nu=0.15$ as indicated in the figure.

From the result of the multiparticle tracking we observe that (1) the beam size does not depend sensitively on $\eta_s$, in particular for the case of small $T_\epsilon$, (2) for small $\eta$, $M_{11}\simeq\epsilon$, (3) $M_{11}$ is blown up rapidly at some $\eta$, (4) for the large $T_\epsilon$ case, the blowup seems to be related to $\eta_s$, (5) the blowup occurs at larger $\eta$ for smaller $T_\epsilon$, and (6) after $\eta$ becomes large enough, the $\eta$ dependence of $M_{11}$ becomes quite smooth and weak. The results of the model illustrate these points, except for point 4: our model is worse for larger $T_\epsilon$. Let us consider this point. (See also the next subsection.)

In the multiparticle tracking, the nominal equilibrium state ($M_{ij}=\epsilon\delta_{ij}$) was used as the initial distribution. Without the radiation, the beam sizes would have been blown up at $\eta$ close to $\eta_s$ due to the resonance overlap. The radiation effect perturbs this structure. The effect of the diffusion is to produce or enhance the stochasticity in the Hamiltonian system. Any regular trajectory is obscured and broadened by $\sqrt{\epsilon}$ after $T_\epsilon$ turns. Small stochastic regions originally separated by the Kol'mogorov-Arnol'd-Moser (KAM) curve[37] can be connected by this mechanism. This radiation diffusion thus can be regarded as enlarging the Hamiltonian stochastic region and enhancing the diffusion rate. On the other hand, the damping effect also affects the Hamiltonian dynamics. It weakens or breaks the resonances. When $\lambda$ [$=\exp(-2/T_\epsilon)$] is slightly smaller than 1, the separatrix around the resonance becomes an unstable limit cycle and the center of the resonance (elliptic fixed point) becomes the sink. When $\lambda$ becomes smaller than some value, the limit cycle shrinks to the sink and the sink becomes unstable. As a whole, the radiation effect breaks the ordered structure of the phase space (i.e., resonances).

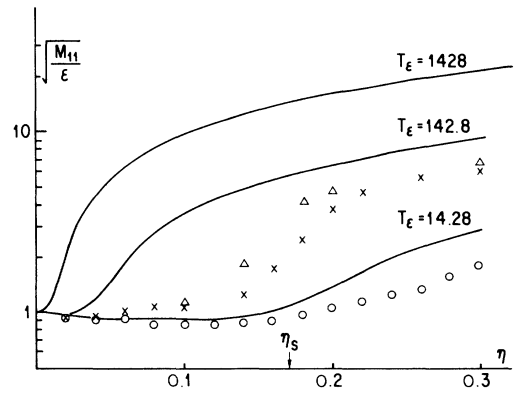


FIG. 10. The beam size of the weak beam as a function of $\eta$ for three values of $T_\epsilon$ and $\nu=0.15$. Solid lines are results of the model. Symbols $\triangle$, $\times$, and $\circ$ show the multiparticle tracking results for $T_\epsilon=1428$, 142.8, and 14.28, respectively.

As is clear from its construction, our model is indifferent to the resonance structure. The resonance occurs through the behavior of an individual particle, which we ignored almost completely. As discussed in the above, resonance structure becomes less important for a stronger radiation effect. It is thus expected that our model becomes more accurate for small $T_\epsilon$. In fact, the numerical agreement becomes better for smaller $T_\epsilon$.

Point 6 is remarkable. It seems to be contrary to the naive consideration that when $\eta$ is large the Hamiltonian dynamics will be strong so that the distribution function will be much different from Gaussian. Point 6, however, implies a possibility that the Gaussian approximation becomes good again for large $\eta$. It can be understood as follows. When $\eta$ is much larger than $\eta_s$ the phase space is filled with the stochastic region even without the radiation effect. It is possible then, that the distribution function has little structure and can be approximated by Gaussian. In fact, the Hamiltonian stochasticity can sometimes be treated as a source at diffusion.[6] In this connection, see Appendix B.

### D. Unphysical increase of the beam sizes

When we compare the results of our model to those of the multiparticle tracking, it is easily seen that our model always overestimates the beam sizes. This comes from the Gaussian approximation.

As shown in Appendix A, $\det M^{\pm}$ changes under **B**. The change is positive except for physically meaningless $R^{\pm}$ ($R^{\pm 1}\lesssim 265$ which means the beam shrinks quite a lot). The change of $\det M$ itself is natural and justified for nonlinear mappings: $\det M$ seems to be invariant only under linear symplectic mapping. Now, however, we use the Gaussian approximation where the entropy $S$ is expressed in terms of $\det M$ as shown in Eq. (B11). As shown in Appendix B, the entropy $S$ should not be changed under symplectic transformation such as **B**. Thus $S$ suffers from an unphysical increase. Under nonlinear mapping, Gaussian $\psi$, if any, produces a non-Gaussian detailed structure. When we approximate $\psi$ as Gaussian, we lose all the information regarding the distribution function except for $M_{ij}^{\pm}$. Any approximation implies the loss of information, which implies the unphysical increase of the entropy. The increase of $S$ means additional diffusion. This, roughly speaking, implies additional heating. This causes unphysical increase of the beam size.

Our $M_{ij}$ has thus some unphysical part. The unphysical part is smaller for smaller $T_\epsilon$. (This is verified by multiparticle tracking.) The reason is that the unphysical diffusion becomes small relative to diffusions from the radiation effect. It is clear, on the other hand, that our model cannot apply to proton rings ($T_\epsilon\to\infty$); there will be no fixed point.

Such an unphysical increase of $S$ seems inevitable when we treat $\psi$ with any approximation. If, however, we could incorporate higher-order moments, for example, the unphysical part of the beam size will become smaller.

It seems very plausible that there exist a functional of $\psi_+$ and $\psi_-$ which tends to be minimum under the map-

pings. Then, what we did is to find its minimizing functions within the Gaussian form in the same manner as applying the variational method. There exists such a functional in the case of the autonomous system (the free energy as shown in Appendix B). If we could find such a functional for a time-dependent system, or even only show its existence, it would be quite valuable and helpful for accelerator theory.

### E. Linear approximation of the beam-beam force

When the force is approximated only by the linear term, the Gaussian approximation becomes fully justified. The kick **B** becomes

$$X'=X, \quad P'=P-K_{\pm}\frac{X}{2M_{11}^{\mp}} , \tag{7.12}$$

so that the mapping **B** becomes

$$\begin{aligned} &M_{11}^{\pm\prime}=M_{11}^{\pm}, \quad M_{12}^{\pm\prime}=M_{12}^{\pm}-K_{\pm}\frac{M_{11}^{\pm}}{2M_{11}^{\mp}} , \\ &M_{22}^{\pm\prime}=M_{22}^{\pm}-K_{\pm}\frac{M_{12}^{\pm}}{M_{11}^{\mp}}+K_{\pm}^2\frac{M_{11}^{\pm}}{(M_{11}^{\mp})^2} . \end{aligned} \tag{7.13}$$

The numerical tracking for $M_{ij}^{\pm}$ seems to show a rich dynamical behavior, period-doubling bifurcation, etc. There is also period-one fixed point[38] with $R\neq 1$ but unstable.[39] The dynamics of this case, despite its appearance, is quite nonlinear since the mapping itself depends on the moments. We can understand the reason of the qualitative difference between linear and nonlinear cases as follows. From Eq. (7.13), it is clear that when one beam is blown up, it feels more beam-beam force, quite contrary to the case given thus far. This model is interesting from a mathematical point of view, but does not seem to illustrate the characteristic features of the beam-beam phenomena.

We can conclude that the nonlinearity plays an important and indispensable role not only in the actual beam-beam phenomena, but also in our model.

### F. Coherent dipole mode

We have not incorporated the dipole mode. It seems a little difficult to incorporate it analytically. For example, the integral $\langle F^2\rangle$ is difficult to evaluate.

Inclusion of the dipole mode, however, is important. (1) According to the multiparticle tracking result of Piwinski,[3] the small separation of beams by the electrostatic separator strongly affects the beam size (so that reduces the lifetime of the beam). It is desirable to understand this phenomenon in order to estimate how much should we separate the beams and how fast the electric field should be decreased. (2) We kick the beam in rf frequency to measure the beam-beam tune shift. (see Refs. 14–18). The kick should be a little large in order to obtain a clear observation. It can affect the beam sizes so that it affects the tune shift. It is also important to understand this effect.

### G. Summary and future problem

A simple model is constructed. All of the points stated in the Introduction are included and have been shown to be necessary. Our model consists of, essentially, approximating the distribution functions as Gaussian. By this, the system of the mapping equations can be closed within the second-order moments, which, however, causes the unphysical increase of the beam sizes and indifference to the nonlinear resonances. These minor points become less serious when we go to "asymptotic utopia ($T_\epsilon\rightarrow 0$)" where the radiation effect beats the Hamiltonian structure. In this respect, our model deals with the asymptotic utopia. Although the actual rings do not live in this utopia, this extreme situation is useful to understand the essential features of the $e^+e^-$ rings. In addition, we did some drastic simplification: (1) reduction of the degree of freedom to one dimension (round-beam limit and flat-beam limit), in particular (2) neglect of horizontal-vertical coupling and synchrotron-betatron coupling, (3) neglect of other sources of nonlinearity and the effect of the physical aperture and so on. These effects are certainly important in operation of the actual storage rings. These are, at the same time, secondary factors for the beam-beam phenomena. Even without such effects there will be the beam-beam phenomena.

In order to obtain quantitatively accurate estimations on the beam behavior, the realistic multiparticle tracking seems to be the most reliable, though we cannot obtain conceptual understanding only from it. Our Gaussian model can illustrate only gross qualitative features. Although too simple and limited, we can acquire a rough understanding on the nature of the beam-beam phenomena by this model. This is what is expected for such a simple model. To be more precise, we must use more parameters to fit the distribution functions and incorporate the secondary factors.

There remains much to do: (1) estimate the unphysical part of the beam sizes, (2) find a method less sensitive to the unphysical increase of the entropy, (3) find the functional stated in Sec. VII D, (4) go beyond the Gaussian approximation (the evaluation of the beam-beam force will be the most difficult point), (5) allow inclusion of the dipole motion, (6) incorporate horizontal and vertical degrees of freedom at the same time, and so on.

In a sense, the beam-beam interaction is a special problem, relevant only to the colliding rings. Because of its simplicity, however, the study of this problem will be helpful in acquiring more understanding on beam dynamics in general.

## ACKNOWLEDGMENTS

The author wishes to thank Professor T. Suzuki and Professor K. Yokoya for detailed discussions. S. Kamada and Dr. K. Oide are acknowledged for helpful comments. Thanks are also due to Professor T. Nishikawa and Professor Y. Kimura for encouragements. He is also indebted to Dr. M. Furman and Dr. K. Y. Ng for valuable information.

## APPENDIX A: DERIVATION OF THE PERIOD-ONE FIXED POINT

In this appendix we show how to derive the formulas for the period-one fixed point $\bar{M}_{ij}$, Eqs. (3.9)–(3.11), for the $\mathbf{B}\rightarrow\mathbf{R}\rightarrow\mathbf{O}$ mappings discussed in the text. For the sake of brevity we pay attention only to $M_{ij}^{+}$ so that we can omit the indices $\pm$: $K\equiv K_{+}$, $A\equiv A(R)$, and so on. For $M_{ij}^{-}$, replace $R$ with $R^{-1}$. Let us first note that $\det M$ and $\mathrm{Tr}M$ are invariant under **O**, while $M_{11}$ is invariant under **B** and **R**. It is thus convenient to work with these three quantities. We thus have

**B**: $\det M'=\det M+K^2(B-A^2)$ ,

$\mathrm{Tr}M'=\mathrm{Tr}M+2KAM_{12}/M_{11}+K^2B/M_{11}$ ,

$M'_{11}=M_{11}$ .

**R**: $\det M''=\lambda^2\det M'+(1-\lambda^2)M'_{11}\epsilon$ ,

$\mathrm{Tr}M''=\mathrm{Tr}M'+(1-\lambda^2)(\epsilon-M'_{22})$, $M''_{11}=M'_{11}$ .

**O**: $\det M'''=\det M''$, $\mathrm{Tr}M'''=\mathrm{Tr}M''$ ,

$M'''_{11}=M''_{11}\cos^2\mu+M''_{22}\sin^2\mu+2M''_{12}\sin\mu\cos\mu$ .

Letting $M'''=M$ and eliminating $M'$ and $M''$ from these expressions, we can obtain equations for $M_{ij}$. From **R** and **B** we obtain

$$(1-\lambda^2)(M_{11}M_{22}-M_{12}^2)=K^2\lambda^2(B-A^2)+(1-\lambda^2)\epsilon M_{11} \tag{A1}$$

and

$$(1-\lambda^2)M_{11}(M_{22}-\epsilon)=\lambda^2(2KAM_{12}+K^2B) , \tag{A2}$$

which imply

$$(1-\lambda^2)M_{12}^2-2KA\lambda^2M_{12}-K^2\lambda^2A^2=0 . \tag{A3}$$

We thus find

$$M_{12}=\frac{\lambda}{1-\lambda^2}(\lambda\pm1)KA . \tag{A4}$$

Since $M_{12}$ decreases by **B**, it should be positive before **B**. We thus take the minus sign. Thus

$$M_{12}=\frac{-\lambda}{1+\lambda}KA , \tag{A5}$$

which is Eq. (3.10). We substitute this into Eq. (A2) to obtain

$$M_{22}=\epsilon+K^2\frac{\lambda^2}{1-\lambda^2}\left[B-\frac{2\lambda}{1+\lambda}A^2\right]\frac{1}{M_{11}} . \tag{A6}$$

This is Eq. (3.11).

Now from **O** we can easily obtain

$$M_{11}=\lambda^2(M_{22}-\epsilon)+\epsilon+\lambda^2\left[2KA\frac{M_{12}}{M_{11}}+K^2B\frac{1}{M_{11}}\right]+\frac{2\lambda}{\tan\mu}\frac{1}{1+\lambda}KA . \tag{A7}$$

From this with Eq. (A5) and Eq. (A6) we have

$$M_{11}^2-2DM_{11}-E=0 , \tag{A8}$$

where $D$ and $E$ are defined in the text. Since $M_{11}$ should be positive, we obtain, Eq. (3.9),

$$M_{11}=D+\sqrt{D^2+E} , \tag{A9}$$

which completes the derivation.

## APPENDIX B: ENTROPY OF THE DISTRIBUTION

The concept of the entropy is quite useful for electron (positron) rings. In this appendix we present some of the characteristic points of the entropy.

It is convenient to start with the autonomous Hamiltonian systems perturbed by the radiation effect. We can thus ignore the difficulty resulting from point 1. We will first recapitulate some of the results of Ref. 9. Then the Gaussian approximation will be applied to some simple case.

When the classical Hamiltonian $H$ is autonomous the behavior of $\psi$ can safely be described by the Fokker-Planck equation

$$\frac{\partial\psi}{\partial\theta}=[H,\psi]+\frac{\partial}{\partial P}(\beta P\psi)+D\frac{\partial^2\psi}{\partial P^2} , \tag{B1}$$

where $\beta=(\pi T_\epsilon)^{-1}$, $D=\beta\epsilon$ and $[\ ,\ ]$ is the Poisson bracket. It is well known that the Fokker-Planck equation has an equilibrium solution

$$\psi(X,P)=\frac{1}{Z}\exp\left[-\frac{H}{\nu\epsilon}\right] ,$$
$$Z=\int dX\,dP\exp\left[-\frac{H}{\nu\epsilon}\right] . \tag{B2}$$

If we denote $\nu\epsilon$ as "temperature" $T$, Eq. (B2) can be regarded as the Boltzmann distribution. It should be noted here that the Boltzmann formula makes sense only when $H$ is positive at infinity. In fact, $Z$ diverges otherwise.

Note that the exact equilibrium solution, Eq. (B2), of the Fokker-Planck equation is characterized by the minimizing function (with constant $T$) of the free energy $F[\psi]$, a functional of $\psi$:

$$F=E-TS , \tag{B3}$$

$$E=\langle H\rangle , \tag{B4}$$

$$S=-\langle\ln\psi\rangle , \tag{B5}$$

where $\langle\ \rangle$ is the average (expectation value)

$$\langle f\rangle=\int dX\,dP\,f(X,P)\psi(X,P)$$

for any function $f$. The proof is simple: we make an infinitesimal variation of $\psi$, $\delta\psi$ with the normalization fixed so that

$$\int dX\,dP\,\delta\psi(X,P)=0 . \tag{B6}$$

Now from

$$F=\langle H+T\ln\psi\rangle \tag{B7}$$

we have

$$\delta F=\int dX\,dP\,\delta\psi(H+T\ln\psi)\ . \tag{B8}$$

In order for $F$ to be minimum, the expression in parentheses should be constant. This implies the Boltzmann distribution, Eq. (B2).

Let us consider, as an example, the Hamiltonian

$$H=\tfrac{1}{2}(X^2+P^2)+\frac{K}{8\pi}X^4\ , \tag{B9}$$

where $K$ is a positive constant. As is easily seen when $K<0$ the Hamiltonian system has the separatrix. There can never be an equilibrium state in such a case: all the particles will go to infinity eventually, however wide the bucket is.

It is often useful to approximate $\psi$ as Gaussian. One way is to approximate $H$ in the Boltzmann formula in quadratic form. We, however, can do better when use is made of $F$. Let us employ the Gaussian approximation, Eq. (3.1). Then we have

$$E[\psi]=\frac{\nu}{2}\mathrm{Tr}M+\frac{3}{4}\frac{K}{2\pi}M_{11}^2\ , \tag{B10}$$

$$S[\psi]=\ln(2\pi e)+\tfrac{1}{2}\ln\det M\ . \tag{B11}$$

By demanding

$$\frac{\partial F}{\partial M_{ij}}=0 \tag{B12}$$

we have $M_{12}=0$, $M_{22}=\epsilon$, and

$$M_{11}^2+\frac{2\pi}{3K}\nu M_{11}-\frac{2\pi}{3K}\nu\epsilon=0\ . \tag{B13}$$

Let $\kappa\equiv 3\epsilon K/\pi\nu$ and $m_g\equiv M_{11}/\epsilon$. The positive solution now is

$$m_g=\frac{-1+\sqrt{1+2\kappa}}{\kappa}\ . \tag{B14}$$

The accuracy of the Gaussian approximation result $m_g$ can be examined by comparing it with the exact one

$$m_e=\frac{\int dx\,x^2\exp-\left[\frac{x^2}{2}+\frac{\kappa}{12}x^4\right]}{\int dx\,\exp-\left[\frac{x^2}{2}+\frac{\kappa}{12}x^4\right]}\ . \tag{B15}$$

The results are compared in Fig. 11. The agreement is surprisingly good. If we had approximated $H$ in quadratic term, we would have another "approximation" where

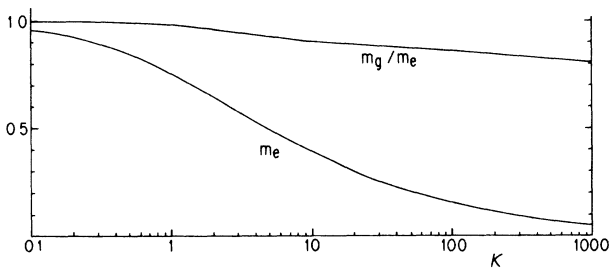


FIG. 11. Comparison between beam sizes from the Gaussian approximation and exact one.

$m$ is always 1. This does not work for large $\kappa$. We thus can conclude that the Gaussian approximation is good as a test function for the minimizing function of $F$. Of course, $F$ is not really minimized by this test function.

Another important property of $S$ is that it does not change under any symplectic transformation, such as the beam-beam force. Imagine the transformation $X_i\to X_i'$, which can be written as

$$X_i'=e^{:A:}X_i\ , \tag{B16}$$

where $X_i$ is a canonical variable, $A$ is the generation function and : : means the Lie transformation.[40] Then $\psi(X_1,X_2)$ transforms to

$$\psi'(X_1,X_2)=\psi(e^{-:A:}X_1,e^{-:A:}X_2)\ , \tag{B17}$$

so that the entropy becomes

$$-\int\psi(e^{-:A:}X_1,e^{-:A:}X_2)\ln\psi(e^{-:A:}X_1,e^{-:A:}X_2)dX_1dX_2\ . \tag{B18}$$

Let us write $e^{-:A:}X_i$ as $\tilde{X}_i$ and note that the Jacobian $\partial(X)/\partial(\tilde{X})$ is 1 from the symplecticity. It is enough to prove the statement. Actually, this property is common to all the quantities defined by $\langle$any function of $\psi\rangle$. Since, however, the entropy can be regarded as the negative information, $S$ is particularly important: No information is lost by the symplectic transformation.

The entropy thus introduced, however, is useless when the Hamiltonian system becomes very chaotic. Of course, $S$ is invariant even in this case. The phase space now is not ordered and $\psi$ becomes quite a singular function. Actually, we can redefine $\psi$ by the coarse graining, which smooths $\psi$ to a regular function. The coarse-grained $\psi$ is more physical, which is just what we can observe. In this case, $S$ should increase due to the coarse graining. The unphysical increase of $S$ due to the Gaussian approximation can partly be interpreted as coming from the coarse graining. In spite of its name, a part of the unphysical increase of $S$ is therefore physical from this point of view.

[1]J. T. Seeman, in *Observations of the Beam-Beam Interaction*, proceedings of the Nonlinear Dynamics Aspects of Particle Accelerators, 1985, edited by J. M. Jowett, M. Month, and S. Turner (Springer, Berlin, 1986).

[2]For example, A. W. Chao, in *Physics of High Energy Particle Accelerators*, proceedings of the Third Annual U.S. Summer School on High Energy Particle Accelerators, Upton and Stony Brook, New York, 1983 edited by M. Month, P. F.

Dahl, and M. Dienes (AIP Conf. Proc. No. 127) (AIP, New York, 1985), p. 201, and references therein.
[3]A. Piwinski, in *11th International Conference on High Energy Accelerators,* Switzerland, 1980, edited by W. S. Newman (Experimentia Supplementum, Vol. 40) (Birkhauser, Basel, 1980), p. 751.
[4]E. Keil, Nucl. Instrum. Methods Phys. Res. **188**, 9 (1981).
[5]S. Myers, Nucl. Instrum. Methods Phys. Res. **211**, 263 (1983).
[6]For example, A. J. Lichtenberg and M. A. Lieberman, *Regular and Stochastic Motion* (Springer, New York, 1983).
[7]For example, in *Nonlinear Dynamics and the Beam-Beam Interaction,* proceedings of the Symposium, Brookhaven National Laboratory, 1979, edited by M. Month and J. C. Herrera (AIP Conf. Proc. No. 57) (AIP, New York, 1979).
[8]F. M. Izraelev, Physica **1D**, 243 (1980).
[9]K. Hirata, Part. Accel. **22**, 57 (1987).
[10]M. H. R. Donald and J. M. Paterson, IEEE Trans. Nucl. Sci. **26**, 3580 (1979).
[11]K. Hirata, KEK Report No. 86-5, 1986 (unpubished).
[12]K. Hirata, Phys. Rev. Lett. **58**, 25 (1987); **58**, 1798(E) (1987).
[13]K. Hirata, KEK Report No. 86-102, 1987 (unpublished).
[14]A. Piwinski, IEEE Trans. Nucl. Sci. **NS-26**, 4268 (1979).
[15]R. Talman, in *Physics of Particle Accelerators,* proceedings of the Fifth Annual U.S. Particle Accelerator School, SLAC, 1985; and selected lectures at the Fourth School, Fermilab, 1984, edited by M. Month and M. Deines (AIP Conf. Proc. No. 153) (AIP, New York, 1987).
[16]R. Talman, ICFA Beam Dynamics Newsletter, 1987 (to be published).
[17]K. Hirata, KEK Report No. 87-40, 1987 (unpublished). It is shown that the relation of two tunes for two coherent modes (0 and $\pi$ modes) are given by $\cos 2\pi\nu_\pi = \cos 2\pi\nu_0 - 2\pi\Xi \sin 2\pi\nu_0$.
[18]T. Ieiri, T. Kawamoto, and K. Hirata, Nucl. Instrum. Methods Phys. Res. (to be published).
[19]E. Keil and R. Talman, CERN Report No. CERN-ISR-TH/81-33, 1981 (unpublished).
[20]This point is not essential in practice, since the integrations depend only on $M_{11}$ which remains constant under **B**.
[21]SPEAR Group, IEEE Trans. Nucl. Sci. **20**, 838 (1973).
[22]H. Wiedeman, in *Nonlinear Dynamics and the Beam-Beam Interaction* (Ref. 7).
[23]According to M. H. R. Donald (private communication), such a phenomenon was also observed by SPEAR.
[24]See figures in Hirata (Ref. 12).
[25]R. Tohm, *Stabilité et Morphogénèse: Essai d'une Théorie Générale des Modèles* (Benjamin, New York, 1972).
[26]H. Whitney, Ann. Math. **62**, 374 (1955); Tohm
[27]J. M. T. Tohompson, *Instabilities and Catastrophes in Science and Engineering* (Wiley, New York, 1982).
[28]E. C. Zeeman, *Catastrophe Theory* (Addison-Wesley, Reading, MA, 1977).
[29]See Hirata (Refs. 12 and 13).
[30]S. Peggs and R. Talman, Phys. Rev. D **24**, 2379 (1981); Talman (Ref. 15).
[31]This can be done exactly for the Gaussian distribution of any aspect ratio and without recourse to the flat-beam limit approximation. See M. Basseti and M. Gygi-Hanney, CERN LEP report No. 221, 1980 (unpublished). The present result agrees with theirs within 85% accuracy for $R = 1$.
[32]The saturated value $\Xi_\infty$ for the flat-beam limit is a little larger than the round-beam case. This is due to the fact that the force is weaker as the beam becomes flat.
[33]J. F. Schonfeld, Ann. Phys. (N.Y.) **160**, 149 (1985); **160**, 194 (1985); **160**, 241 (1985); in *Nonlinear Dynamics Aspects of Particle Accelerators,* edited by J. M. Jowett, M. Month, and S. Turner (Lecture Notes on Physics, Vol. 247) (Springer, Berlin, 1986).
[34]S. Kheifets, Part. Acc. **15**, 153 (1984).
[35]F. Ruggiero, Ann. Phys. (N.Y.) **153**, 122 (1984); Report No. CERN 86-06, 1986 (unpublished).
[36]K. Takayama, KEK Report No. KEK 80-13, 1981 (unpublished).
[37]The KAM theory is reviewed in Lichtenberg and Lieberman, *Regular and Stochastic Motion* (Ref. 6).
[38]M. Furman (private communication).
[39]K. Y. Ng (private communication).
[40]A. J. Dragt, in *Physics of High Energy Particle Accelerators,* proceedings of the Summer School on High Energy Particle Accelerators, Fermilab, 1981, edited by R. A. Carrigan, F. R. Huson, and M. Month (AIP Conf. Proc. No. 87) (AIP, New York, 1982), p. 147.